Efficient Antenna Systems: DSS 14 64-Meter-Diameter Antenna Polarization Properties

P. D. Potter
Communications Elements Research Section

The polarization clock angle of a linearly polarized paraboloidal antenna is a function of both its secondary pattern characteristics and the pointing error relative to the antenna axis of revolution. For polarization tracking scientific experiments such as those planned in support of Project Helios, it is necessary to have an understanding of the relationship between the feed system polarization clock angle (a physically measured quantity) and the overall antenna polarization clock angle. In particular, the S- and X-band reflex feed system introduces significant antenna beam asymmetry which gives rise to polarization error. In this reporting, the DSS 14 64-m antenna secondary pattern characteristics are developed as a function of the reflex feed characteristics previously reported. The polarization angle error is computed as a function of antenna pointing error, typical antenna open-loop pointing errors are reviewed, and the expected polarization distortion is given.

I. Analysis

The coordinate system selected for the secondary pattern analysis is a standard right-handed rectangular system, as shown in Fig. 1. Completely general expressions for the far-field polar and azimuthal pattern components are (Ref. 1)

$$E_\theta(\theta,\phi) = \sum_M E_{\theta me}(\theta)\sin(m\phi) \quad \text{(even)} + \sum_M E_{\theta mo}(\theta)\cos(m\phi) \quad \text{(odd)} \tag{1a}$$

$$E_\phi(\theta,\phi) = \sum_M E_{\phi me}(\theta)\cos(m\phi) \quad \text{(even)} + \sum_M E_{\phi mo}(\theta)\sin(m\phi) \quad \text{(odd)} \tag{1b}$$

From geometry, the rectangular field components are given by

$$E_X(\theta,\phi) = E_\theta(\theta,\phi)\cos\theta\cos\phi - E_\phi(\theta,\phi)\sin\phi \tag{2a}$$

$$E_Y(\theta,\phi) = E_\theta(\theta,\phi)\cos\theta\sin\phi + E_\phi(\theta,\phi)\cos\phi \tag{2b}$$

In general, the antenna response in a particular θ, ϕ direction is elliptically polarized; this response is conveniently described by a polarization ellipse, as shown in Fig. 2. At a given point in space, the X- and Y-field components can be expressed as follows:

$$E_X(\theta,\phi) \equiv E_{XO}(\theta,\phi)\cos(\omega t) \tag{3a}$$

$$E_Y(\theta,\phi) \equiv E_{YO}(\theta,\phi)\cos(\omega t + \delta) \tag{3b}$$

where ω is angular frequency and t is time.

From geometry (Fig. 2):

$$E_U(\theta,\phi) = E_X(\theta,\phi)\cos\tau + E_Y(\theta,\phi)\sin\tau \quad (4a)$$

$$E_V(\theta,\phi) = -E_X(\theta,\phi)\sin\tau + E_Y(\theta,\phi)\cos\tau \quad (4b)$$

With some algebraic manipulation (Ref. 2) it is found that

$$\tau = \frac{1}{2}\arctan\left[\frac{2E_{XO}(\theta,\phi)\times E_{YO}(\theta,\phi)\times\cos\delta}{E_{XO}^2(\theta,\phi) - E_{YO}^2(\theta,\phi)}\right] \quad (5)$$

It is assumed that the feedhorn input is linearly polarized at a clock angle β. By linearity, the overall vector antenna pattern $E_T(\theta,\phi,\beta)$ is given by

$$\mathbf{E}_T(\theta,\phi,\beta) = \mathbf{E}_1(\theta,\phi)\sin\beta + \mathbf{E}_2(\theta,\phi)\cos\beta \quad (6)$$

where

$\mathbf{E}_1(\theta,\phi)$ is the antenna pattern for $\beta = 90$ deg (7a)

and

$\mathbf{E}_2(\theta,\phi)$ is the antenna pattern for $\beta = 0$ deg (7b)

The assumption is now made that $|\mathbf{E}_T|$ is independent of β. This assumption is tantamount to assuming that the feedhorn main beam radiation pattern is independent of β, an excellent approximation for the 64-m corrugated feedhorns. It is readily shown that this assumption can only be satisfied by the following conditions:

$$E_{2\phi}(\theta,\phi) = \pm E_{1\theta}(\theta,\phi) \quad (8a)$$

$$E_{2\theta}(\theta,\phi) = \mp E_{1\phi}(\theta,\phi) \quad (8b)$$

where $E_{1\theta}(\theta,\phi)$ and $E_{2\theta}(\theta,\phi)$ are the polar field components of $\mathbf{E}_1(\theta,\phi)$ and $\mathbf{E}_2(\theta,\phi)$, and $E_{1\phi}(\theta,\phi)$ and $E_{2\phi}(\theta,\phi)$ are the azimuthal field components of $\mathbf{E}_1(\theta,\phi)$ and $\mathbf{E}_2(\theta,\phi)$.

Combining (6) and (8):

$$E_\theta(\theta,\phi,\beta) = E_{1\theta}(\theta,\phi)\sin\beta \pm E_{1\phi}(\theta,\phi)\cos\beta \quad (9a)$$

$$E_\phi(\theta,\phi,\beta) = E_{1\phi}(\theta,\phi)\sin\beta \mp E_{1\theta}(\theta,\phi)\cos\beta \quad (9b)$$

For the case of $\phi = \beta$, from (2) and (9),

$$E_X(\theta,\beta) = E_{1\phi}(\theta,\beta)\cos(2\beta) + E_{1\theta}(\theta,\beta)\sin(2\beta) \quad (10a)$$

$$E_Y(\theta,\beta) = -E_{1\theta}(\theta,\beta)\cos(2\beta) + E_{1\phi}(\theta,\beta)\sin(2\beta) \quad (10b)$$

where the $\cos\theta$ factor has been removed from (2) because of the narrow secondary pattern beamwidth, and the upper signs are used in (9).

The functions $E_{1\phi}(\theta,\beta)$ and $E_{1\theta}(\theta,\beta)$ correspond to the "even" modes in (1) and can be readily computed using JPL software. Using (3), (5), and (10), the polarization clock angle τ may be computed. Ideally, τ would equal β, the physically measured polarization quantity. Asymmetry in the reflex feed system, however, introduces a difference between τ and β, i.e., a polarization error.

II. Computed Results

The reflex feed system radiation pattern, in the form of Eq. (1), is already available from previous calculations and 1/7-scale model tests (Refs. 1, 3). Excellent agreement between computed and measured patterns is achieved by using only the $m = 0$ and $m = 2$ asymmetrical components in addition to the nominal, desired $m = 1$ component. Fields scattered by the slightly asymmetrical antenna subreflector can be calculated using the Ludwig scattering program (Ref. 4). It has been previously determined, however, that the pattern asymmetry introduced by the subreflector is minor compared to the asymmetry in the reflex feed system (see Ref. 3, p. 143). In the interest of economy, therefore, a subreflector "symmetrically equivalent" to the actual subreflector was determined. Subreflector patterns were then calculated using an upgraded version of the Rusch scattering program (Ref. 5). This program is extremely fast and economical to use, as it can perform the azimuthal (physical optics) integration analytically (rather than numerically) by virtue of the assumption of a scattering surface of revolution. Professor W. V. T. Rusch (University of Southern California, Consultant to JPL Communications Elements Research Section) originally formulated the scattering program to handle asymmetrical illumination patterns of the form of Eq. (1), but this capability was never utilized. For the polarization problem, the capability was exercised and checked out numerically with Ludwig's flat plate scattering technique (Ref. 4). The ability to perform highly economical scattering calculations of asymmetrically illuminated symmetrical reflectors with the Rusch program is felt to be a powerful new capability.

The three ($m = 0, 1, 2$) azimuthal Fourier component subreflector scattered patterns are shown in Fig. 3. For comparison, the standard corrugated feedhorn patterns are shown in Fig. 4. Figures 5 and 6 show the total (sum of the $m = 0, 1, 2$ components) scattered patterns. As seen in the phase patterns, the $m = 1$ component is symmetrical with respect to the z ($\theta = 0$) axis, whereas the $m = 0$ and 2 components are antisymmetrical (this is also clear from Eq. 1). Slight pattern asymmetry results in the $\phi = 0/180$-deg cut total pattern (Fig. 5). Also, a cross-polarized component arises in the $\phi = 90/270$-deg cut (Fig. 6). These data were used as input to the Rusch program again to

compute the antenna secondary patterns (subreflector scatterings off the paraboloid). Figures 7, 8, 9, and 10 show the secondary patterns analogous to the subreflector patterns in Figs. 3 through 6. The (minor) effect of the 64-m antenna quadripod structure is not included in these patterns.

Using the data shown in Fig. 7 and the analysis developed in the preceding section, the polarization error $(\tau - \beta)$ was computed as a function of the feedhorn polarization clock angle β; the results are shown in Fig. 11. The polarization error is very nearly sinusoidally related to β, with a peak amplitude which is very nearly linearly related to the antenna pointing error θ.

III. 64-Meter-Diameter Antenna Pointing Errors

In February 1973, two days of high-precision Ku-band DSS 14 antenna pointing data were taken by Arthur Niell of the Planetary Atmospheres Section. These data were corrected for station timing and ephemeris errors and then least-squares-fitted to a cubic spline in antenna elevation angle; the result is shown in Fig. 12. Three different radio sources, 3C273, 3C274, and 3C84 were utilized by Niell in his tests. As seen in Fig. 12, the peak pointing errors are 0.010 – 0.020 deg and more typically less than 0.010 deg. These data are ideal, however, since great care was taken to point the antenna properly. Typical open-loop tracking mission pointing is presumably not as good.

IV. Conclusions

From a comparison of the computed polarization errors shown in Fig. 11 with ideal condition antenna pointing errors measured by A. Niell, it appears that proper antenna pointing is critical to the Project Helios polarization rotation experiment, but that if the antenna is properly pointed, the polarization distortion caused by reflex feed can be held within acceptable limits.

References

1. Potter, P. D., "S- and X-Band RF Feed System," in *The Deep Space Network Progress Report*, Technical Report 32-1526, Vol. VIII, pp. 53–60. Jet Propulsion Laboratory, Pasadena, Calif., April 15, 1972.
2. Rusch, W. V. T., and Potter, P. D., *Analysis of Reflector Antennas*, Academic Press, New York, 1970, pp. 61–68.
3. Potter, P. D., "S- and X-Band RF Feed System," in *The Deep Space Network Progress Report*, Technical Report 32-1526, Vol. IX, pp. 141–146. Jet Propulsion Laboratory, Pasadena, Calif., June 15, 1972.
4. Ludwig, A. C., *Calculation of Scattered Patterns from Asymmetrical Reflectors*, Technical Report 32-1430, Jet Propulsion Laboratory, Pasadena, Calif., Feb. 15, 1970.
5. Ludwig, A. C., and Rusch, W. V. T., *Digital Computer Analysis and Design of a Subreflector of Complex Shape*, Technical Report 32-1190, Jet Propulsion Laboratory, Pasadena, Calif., Nov. 15, 1967.

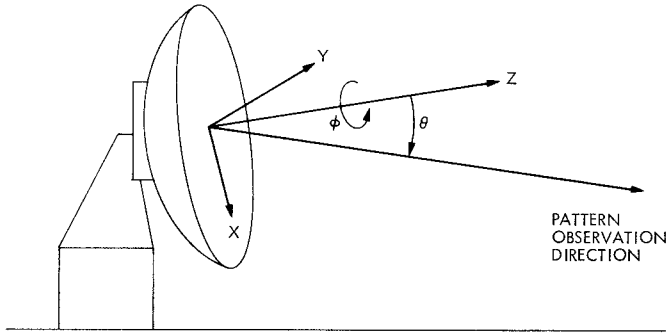

Fig. 1. Antenna pattern coordinate system

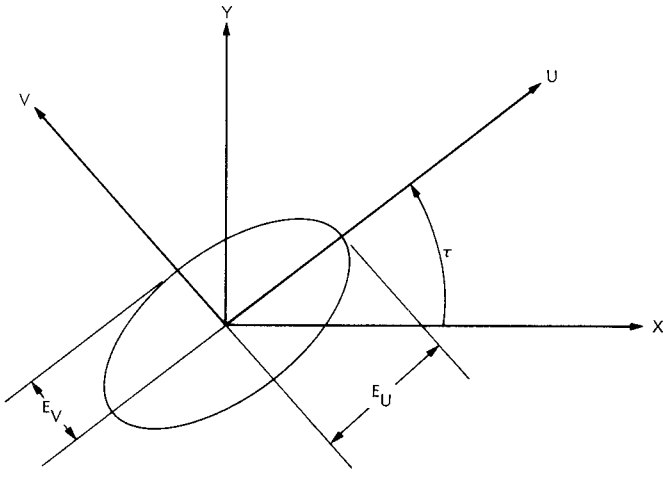

Fig. 2. Polarization ellipse

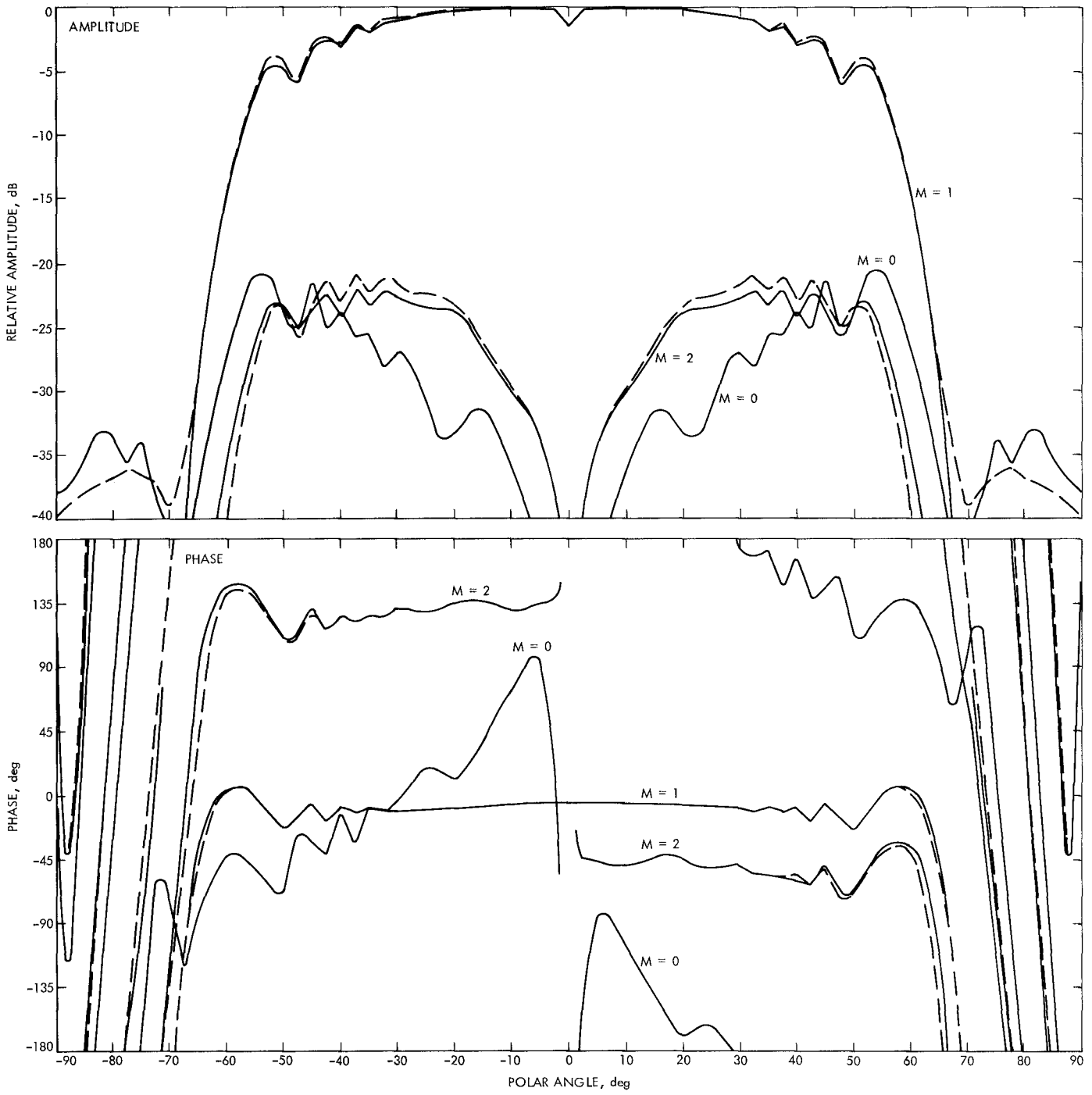

Fig. 3. Reflex feed subreflector scattered azimuthal Fourier component patterns

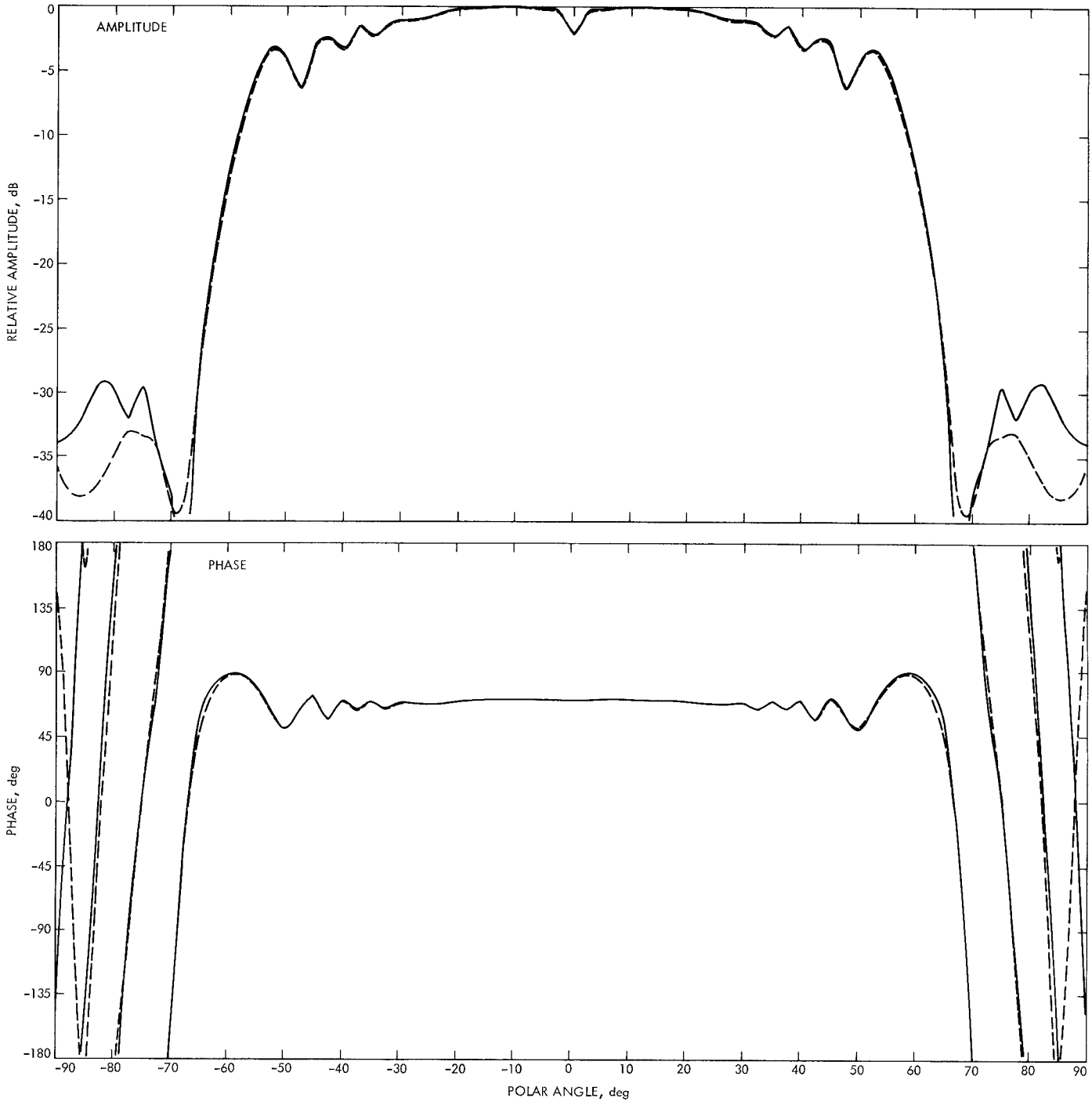

Fig. 4. Standard corrugated feedhorn scattered patterns

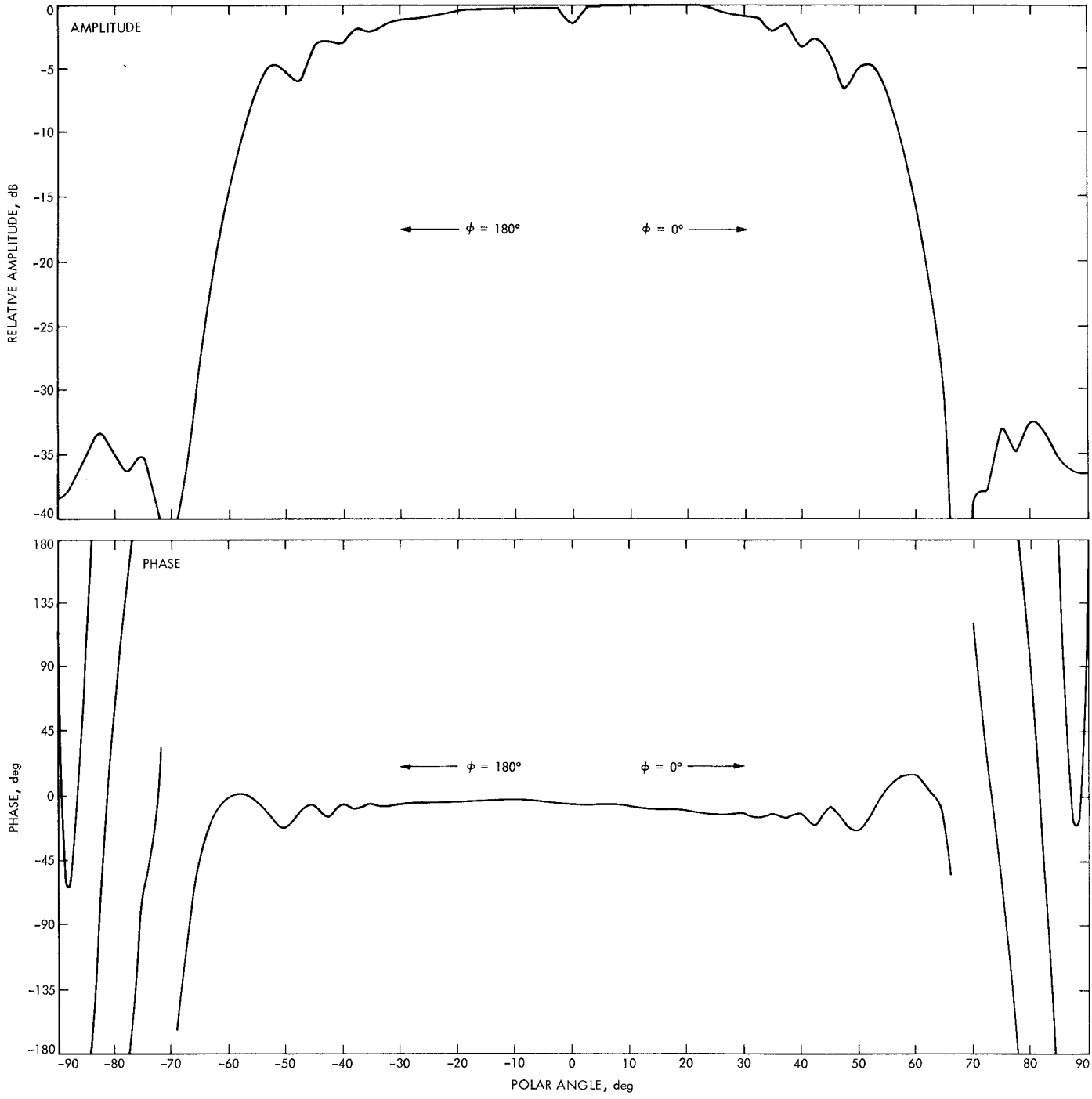

Fig. 5. Total reflex feed subreflector scattered patterns, $\phi = 0/180$-deg cut

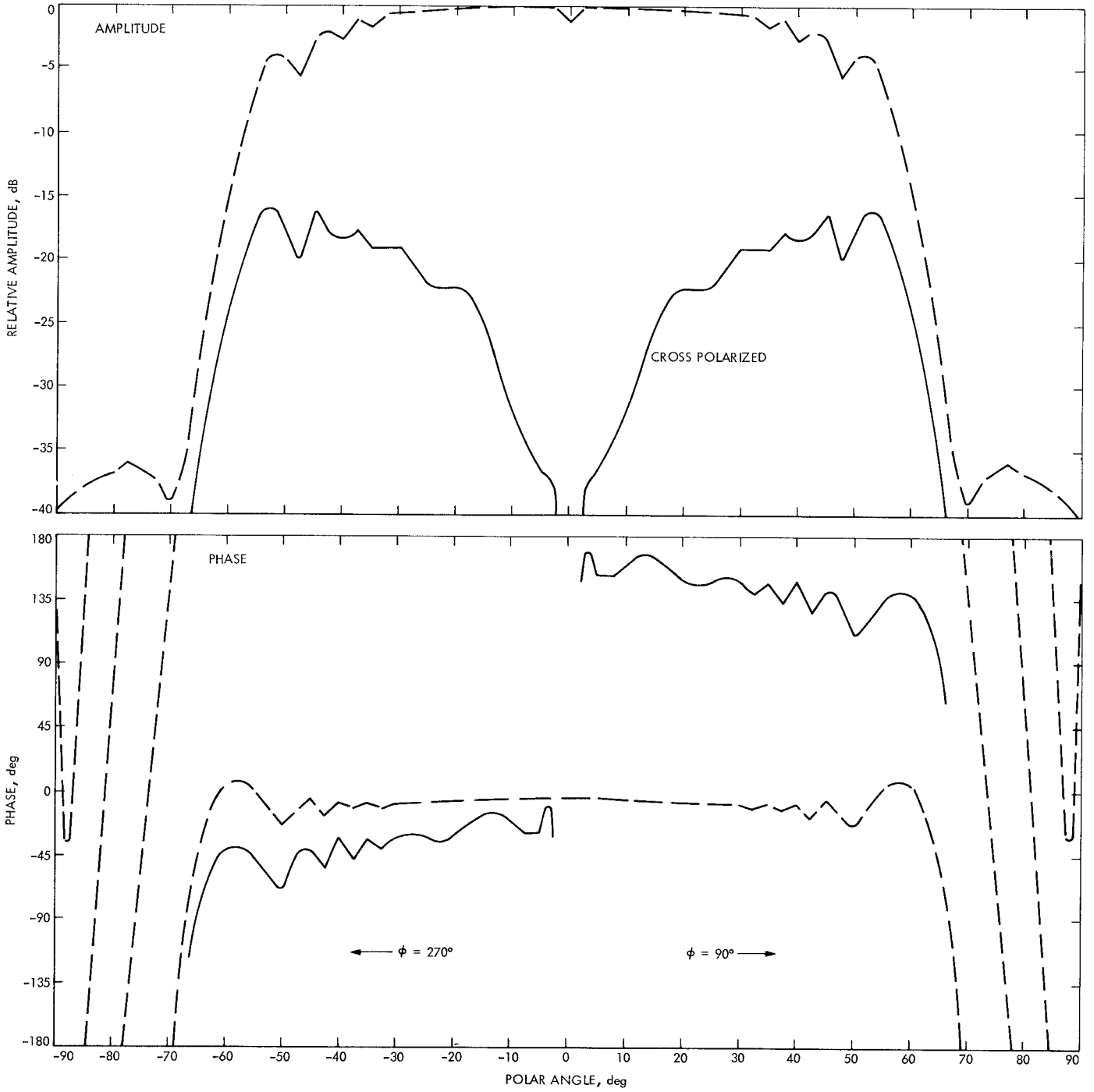

Fig. 6. Total reflex feed subreflector scattered patterns, ϕ = 90/270-deg cut

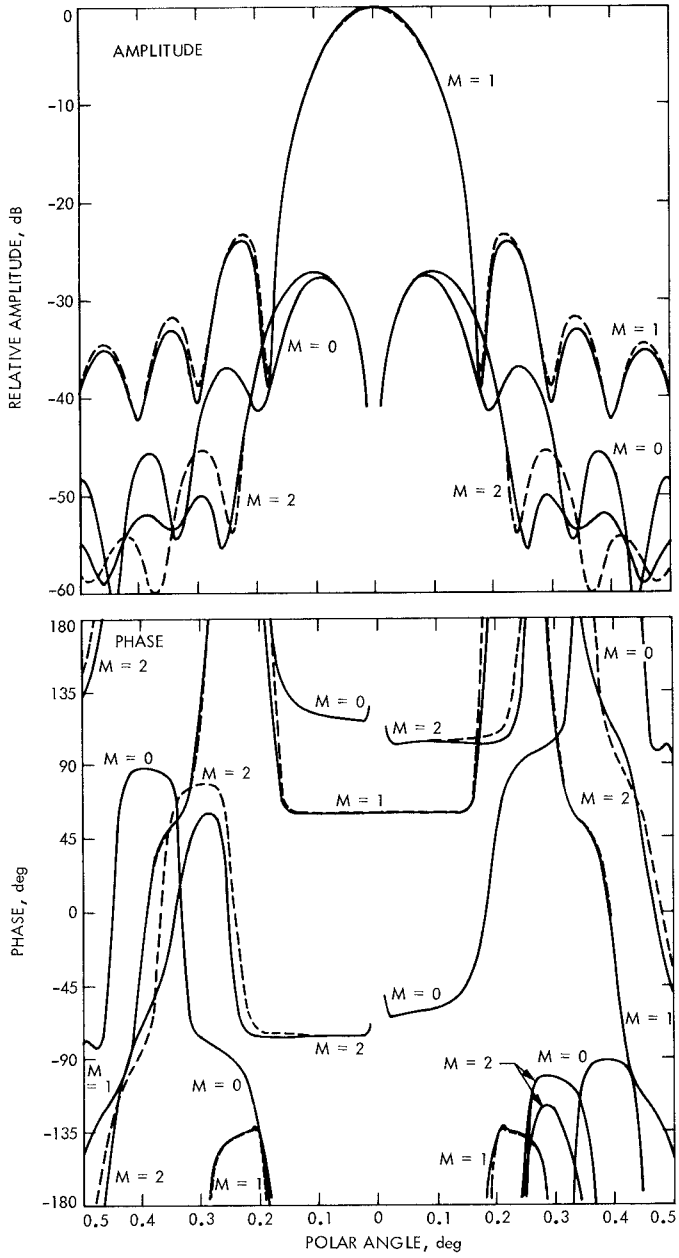

Fig. 7. S-band 64-m paraboloid azimuthal Fourier component patterns, reflex feed, no quadripod

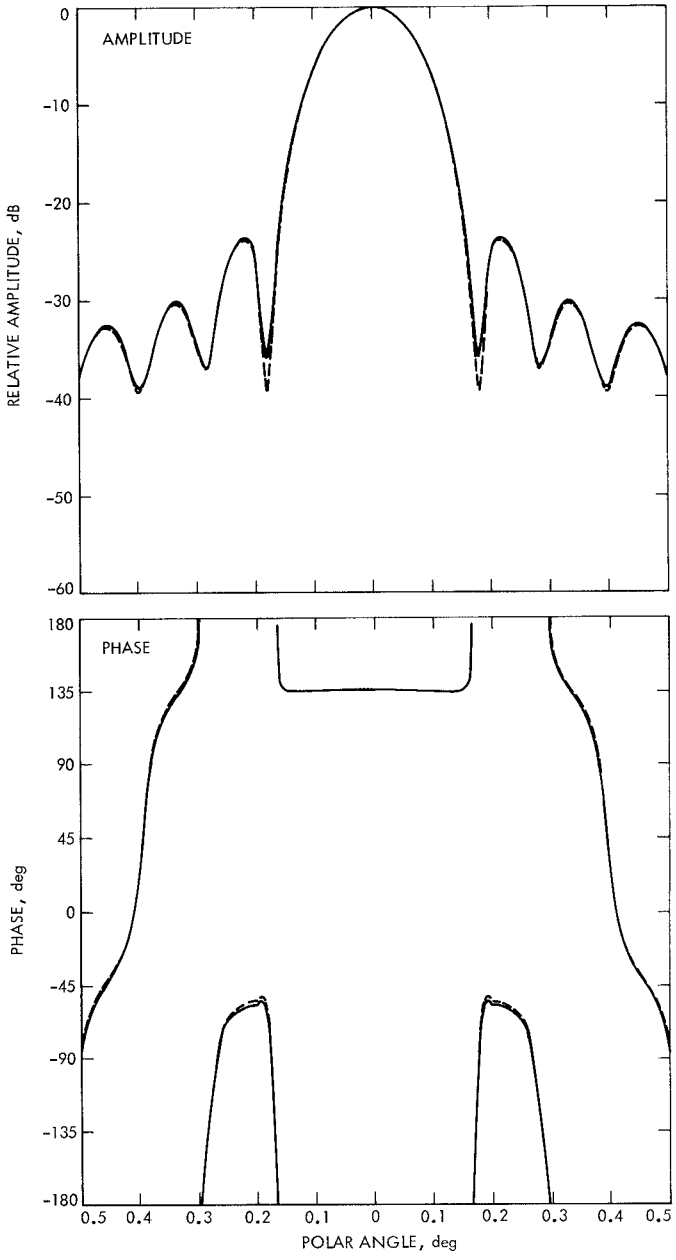

Fig. 8. S-band 64-m paraboloid patterns, standard corrugated feedhorn, no quadripod

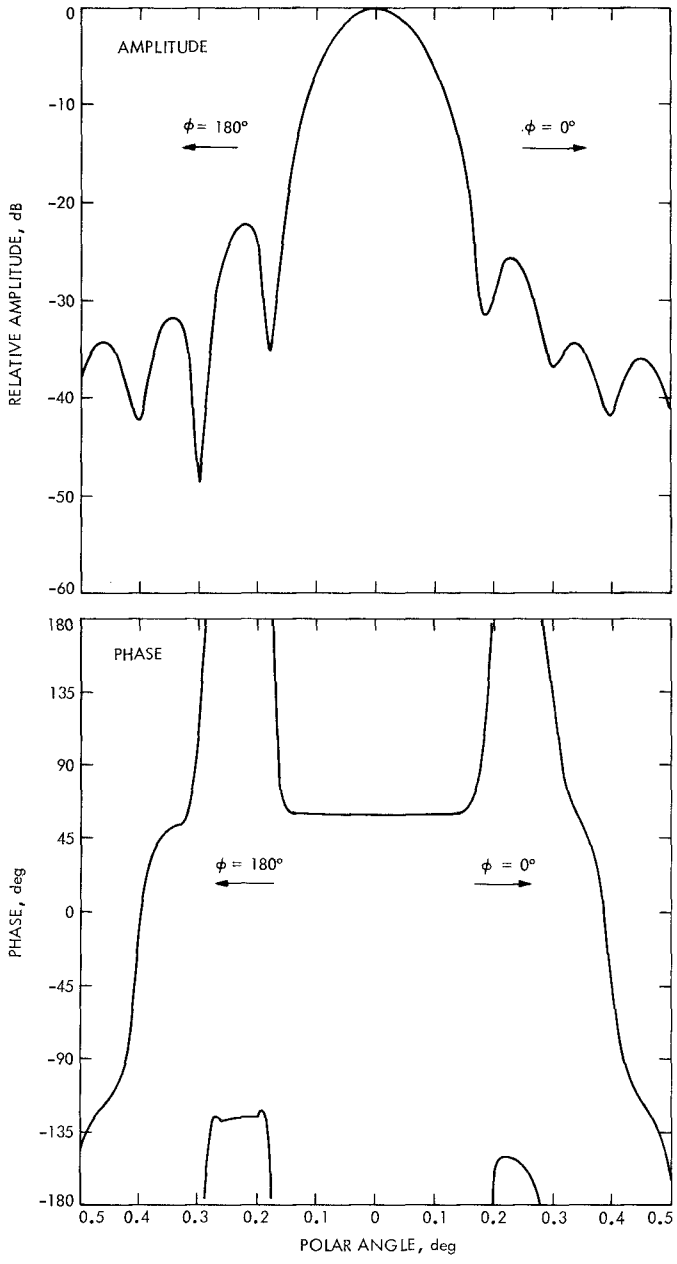

Fig. 9. S-band 64-m paraboloid total patterns, ϕ = 0/180-deg cut, reflex feed, no quadripod

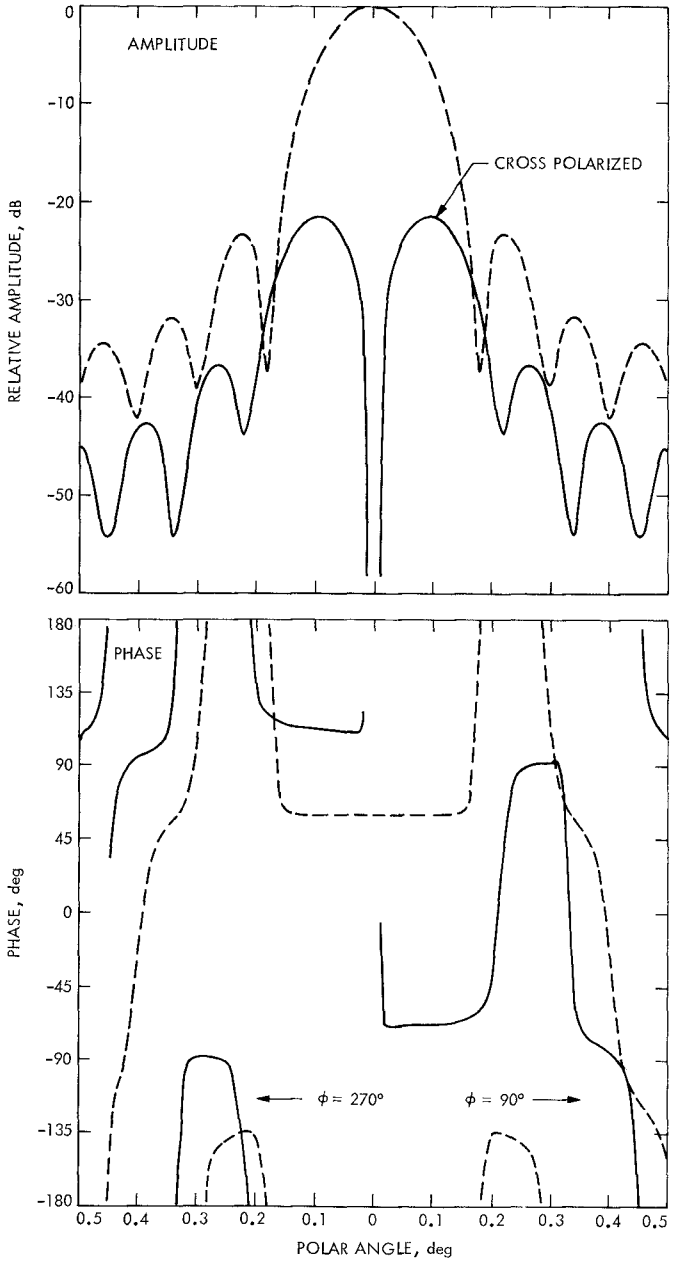

Fig. 10. S-band 64-m paraboloid total patterns, ϕ = 90/270-deg cut, reflex feed, no quadripod

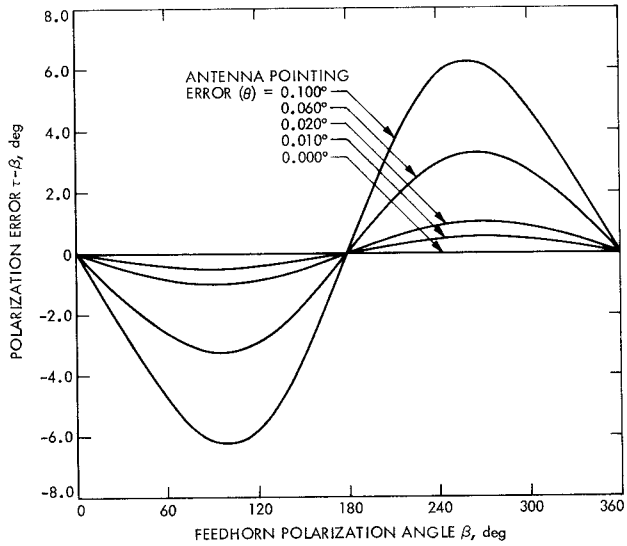

Fig. 11. Polarization error vs feedhorn polarization angle

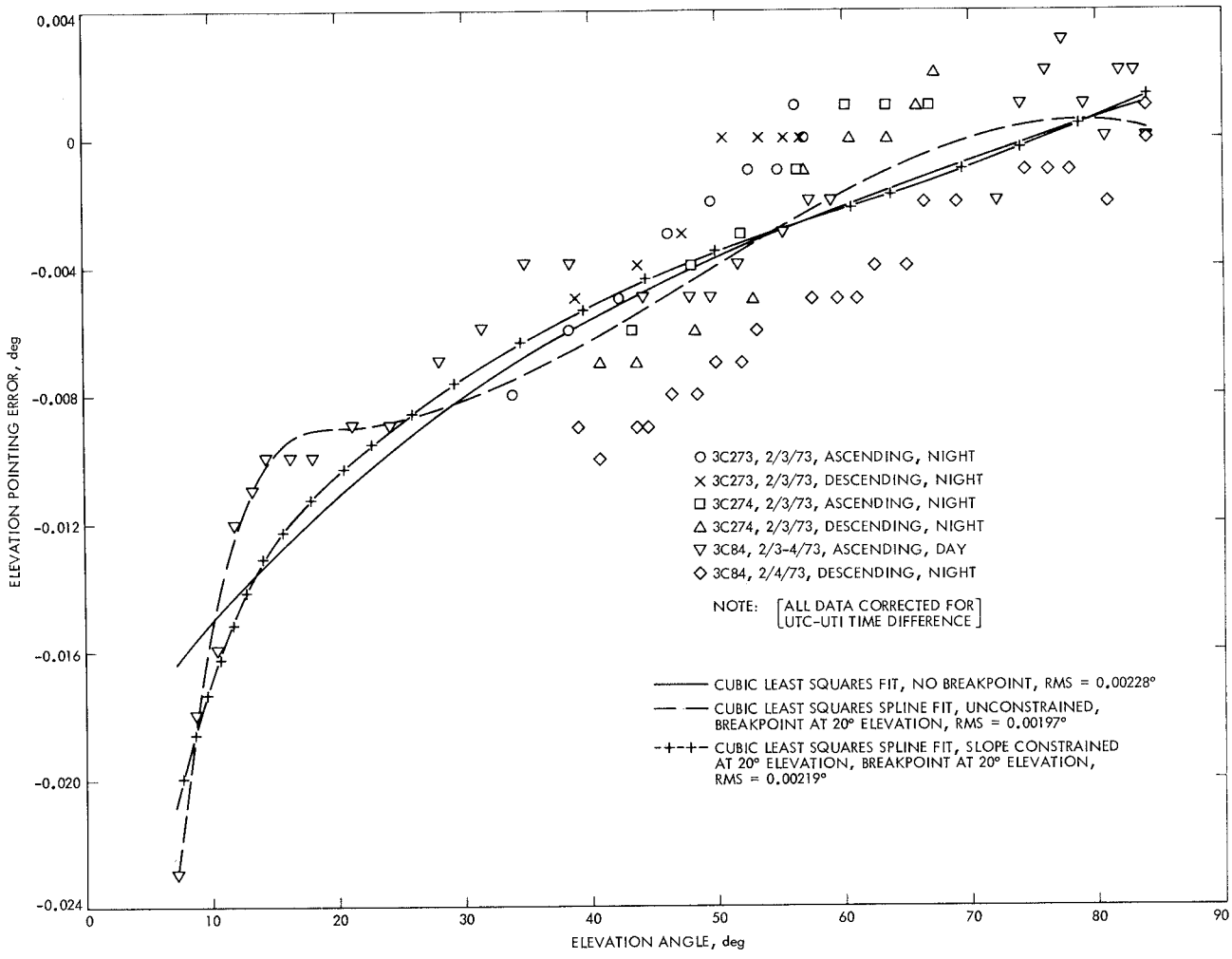

Fig. 12. DSS 14 Ku-band elevation pointing error, February, 1973